

# MULTITRACER METHOD OF DIFFUSION MEASUREMENT IN CHROMIUM-MANGANESE STEELS



PL0500218

Joanna Dudala, Zdzisław Stęgowski, Jolanta Gilewicz-Woźniak

Faculty of Physics and Nuclear Techniques, University of Science and Technology, Al.  
Mickiewicza 30, 30-059 Kraków

**Abstract:** The paper presents an application of multitracer method to diffusion measurement in Cr-Mn steels. Radioisotope tracers of chromium  $^{51}\text{Cr}$ , manganese  $^{54}\text{Mn}$  and iron  $^{59}\text{Fe}$  were used simultaneously in the diffusion process. Gamma-spectrums' measurement and the proper analysis enabled evaluation of concentration distribution for each tracer. As a new tool, artificial neural networks (ANN) method was used for spectrums' analysis. The proper solution of the diffusion model was applied to the experimental tracers' distribution data and diffusion coefficients were determined.

## 1. INTRODUCTION

Selection of the metallic materials used in modern industrial technologies is determined by the conditions in which they are supposed to work. They are often exposed to aggressive atmospheres and high temperatures. Industrial steels, which show high heat – resistance, are composed mainly on the base of iron, chromium and nickel. At present the chromium-manganese steels are the objects of interest due to their lower price and better heat – resistance as well as mechanic properties. The full description of the mechanism of Cr-Mn steels oxidation requires the knowledge of each partial process. For example it should be considered: transport of steel's components in the metallic phase, outward diffusion of steel's components through the scale and inward diffusion of oxidant through the scale. The transport of metals in the metallic phase is supposed to be the slowest partial process, determining the rate of the whole steel oxidation.

The aim of this paper is examination of self-diffusion processes in austenitic Cr-Mn steels in order to evaluate diffusion coefficients of chromium, manganese and iron. The serial sectioning technique was used to evaluate diffusion coefficient of radioisotopes of chromium  $^{51}\text{Cr}$ , manganese  $^{54}\text{Mn}$  and iron  $^{59}\text{Fe}$ . This technique involved electrolytic dissolution of a metallic sample on a filter paper soaked in electrolyte. In experimental procedure the activity distribution on a filter paper as well as the residual activity of the specimen were calculated from gamma-spectrums acquired by a scintillation (NaJ(Tl)) counter. Due to small peak resolution and significant Compton Effect fraction in these spectrums, the artificial neural networks (ANN) were used in their analysis. Diffusion coefficients have been evaluated by applying the solution of the diffusion model (II Fick's law) for a boundary as thin layer geometry and a semi-infinite solid.

## 2. EXPERIMENTAL

Two types of austenitic steels, having the NaCl crystal structure (cubic face centred structure) were used in the experiment. Their composition is given in Table 1. The steels' samples of 14 mm diameter and 1 mm thick were carefully polished and degreased with acetone.

Table 1. Chemical composition of the Cr-Mn steels

Grate of steel	Concentration of elements (% wt.)				
	C	Cr	Mn	Si	Ca
5H17G17 (Cr17Mn17)	0,52	17,40	16,89	-	-
3H13G18S2Ca (Cr13Mn18SiCa)	0,32	12,84	18,82	1,80	0,95

One surface of each sample was coated with a very thin layer of radioactive atoms by the electrolytic reduction of chromium, manganese and iron from the radioactive solutions of the chlorides:  $^{51}\text{CrCl}_3$ ,  $^{54}\text{MnCl}_2$  and  $^{59}\text{FeCl}_3$  (Figure 1a). The diffusion experiment was performed by annealing the prepared samples within evacuated and sealed quartz ampoules at temperature 1173 K. The duration of diffusional annealing was chosen in such a way that the thickness of the sample was greater than the penetration depth of the tracer [1,2]. This allows considering the discussed system in terms of approximation to a semi-infinite solid. The penetration profiles were determined by the serial sectioning method [3,4]. This technique involved electrolytic dissolution of a metallic sample on a filter paper soaked in electrolyte (25 % vol. conc.  $\text{H}_2\text{SO}_4$ , 25 % vol. conc.  $\text{H}_3\text{PO}_4$ , 50 % vol.  $\text{C}_2\text{H}_6\text{O}_2$ ). The apparatus used in this procedure is shown in Fig. 2b. The thickness of each removed section (about  $3\ \mu\text{m}$ ) was determined by gravimetric and direct measurement. The mass of the sample was measured using an analytical balance with the accuracy  $10^{-4}\ \text{g}$ .

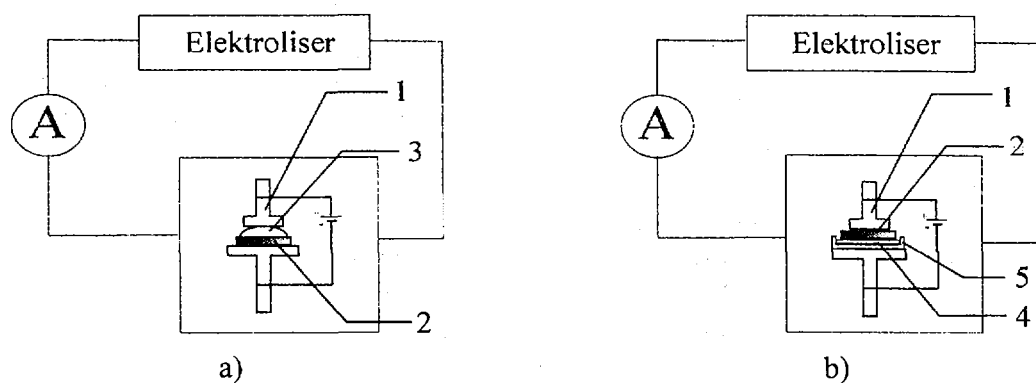
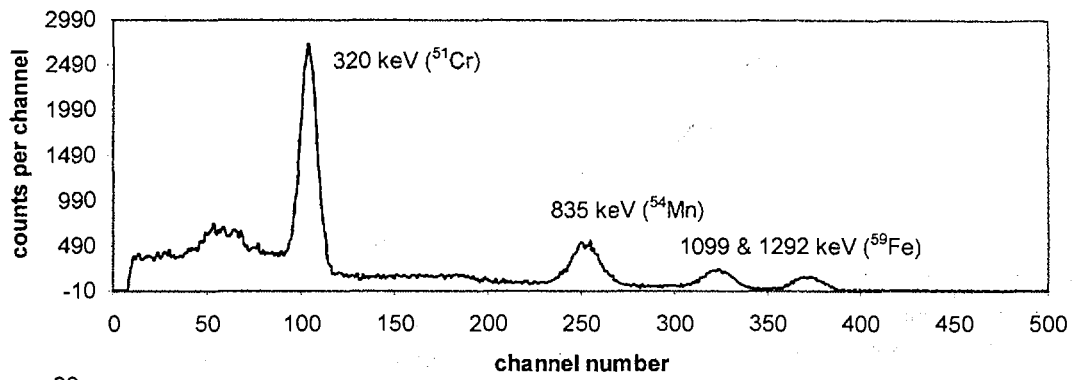
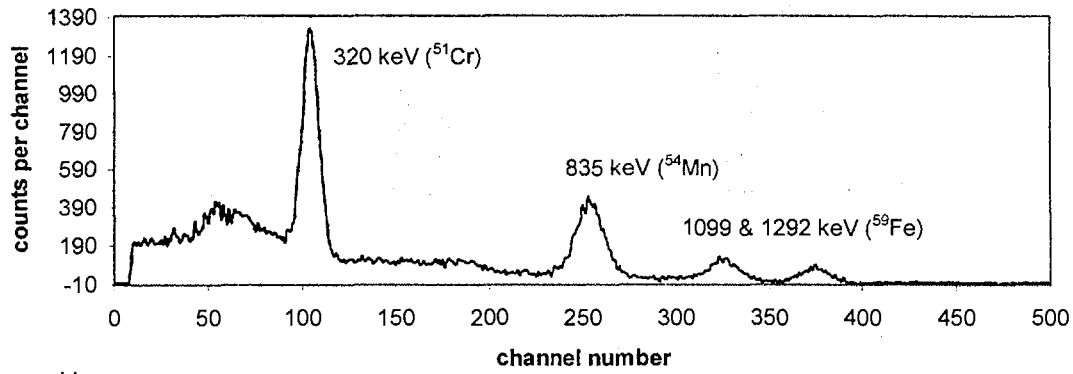


Fig. 1. Apparatus used for: a) electrolytic deposition of radioactive layers on the sample surface; b) anodic dissolution of thin metal layers from the sample surface, 1 – anode, 2 – sample, 3 – radioactive solution of chlorides, 4 – filter paper, 5 – aluminum vessel

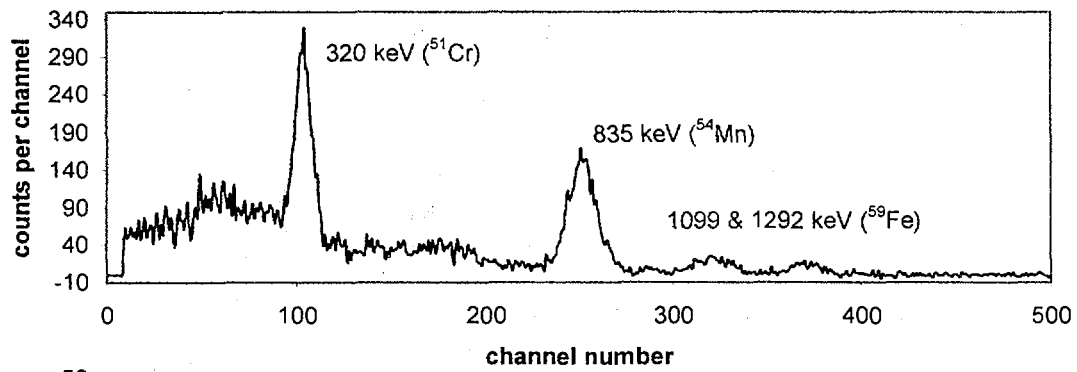
In experimental procedure the gamma-spectrums of the removed layer was acquired using the scintillation ( $\text{NaI(Tl)}$ ) counter combined with the multichannel analyzer (500 channels). The examples of the gamma-spectrums (after background subtraction) for different layers are shown in Figure 2. For deep layers the activities of the tracers were significantly decreased. For the spectrums analysis the artificial neural network was applied.



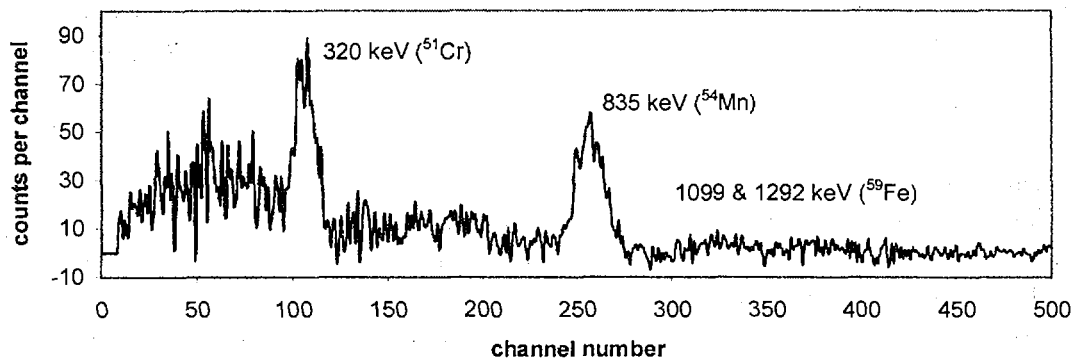
layer - 29



layer - 44



layer - 56



layer - 68

Fig. 2. The examples of the gamma-spectrums for different layers

### 3. SPECTRUM ANALYSIS

#### 3.1. Artificial Neural Networks

Artificial neural networks (ANN) are composed of simple elements (neurons) operating in parallel and serial structure (network). These elements resemble biological nervous systems. As in nature, the network function is determined mostly by the connections between elements. The ANN can be trained to perform a particular function by adjusting the values of the connections (weights) between elements. Commonly, ANN are adjusted (trained) so that a particular input leads to a specific target output. The network is adjusted by comparison of the output and the target, until the network output matches the target. Typically, many such input/target pairs are used to train a network (*sc. supervised learning*). Artificial neural networks have been trained to perform complex functions in various fields of application including prediction, non-linear problems, pattern recognition, identification, classification, speech, vision and control systems.

At present, multiple-layer feed-forward networks with back-propagation learning rule are most common. Generally, the neurons used in each layer may have a linear or nonlinear transfer function. Between the layers, the neurons' transfer functions should be combination of linear and nonlinear. For specific application of ANN, either a network's structure or neurons' transfer functions are selected individually and properly tested in order to choose the best structure

#### 3.2. ANN of the presented method

The main aim of the ANN application in the presented case was evaluation of the activity of chromium  $^{51}\text{Cr}$ , manganese  $^{54}\text{Mn}$ , and iron  $^{59}\text{Fe}$  from gamma-spectrums (Fig. 2.). In this case the input data vector  $\mathbf{X}(x_1, x_2, \dots, x_{500})$  included the count numbers for each spectrum's channel and the output vector  $\mathbf{Y}(y_1, y_2, y_3)$  included the relative activities of the three isotopes. For the network training process, the proper set of input ( $\mathbf{X}$ ) and output (target) data ( $\mathbf{Y}$ ) had been prepared. Some part of the data had been used for network learning and the other part for testing. Dozens of network structures had been tested for the optimal ANN to choose. Finally, it turned out that the one-layer linear network is optimal for the presented aim (see Figure 3.). This network executes the following relation:

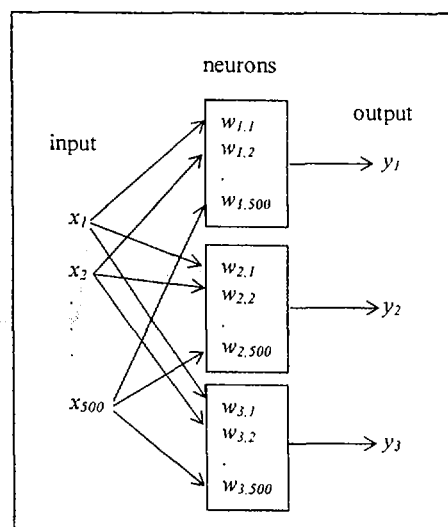


Fig. 3. Structure of ANN

$$\mathbf{Y} = \mathbf{W} * \mathbf{X} \quad (1)$$

where  $\mathbf{W}$  is a (3 , 500) dimensions matrix.

The element values of the matrix  $\mathbf{W}$  should be arranged in such a way that the first row evaluates the activity of chromium  $^{51}\text{Cr}$  ( $y_1$ ) from the spectrum ( $\mathbf{X}$ ), the second and the third evaluates the activity of manganese  $^{54}\text{Mn}$  and iron  $^{59}\text{Fe}$  respectively. Least squares criterion and gradient iteration method have been used for matrix ( $\mathbf{W}$ ) element values calculation [5]. For verification of this method the Ge spectrometer has been used in order to precisely analyze gamma-spectrums of the selected samples (layers). The comparison of the results

from the Ge spectrometer measurement and from the scintillation spectrometer supported by ANN method is shown in Figure 4. Both results show a full conformity in a statistical error limits.

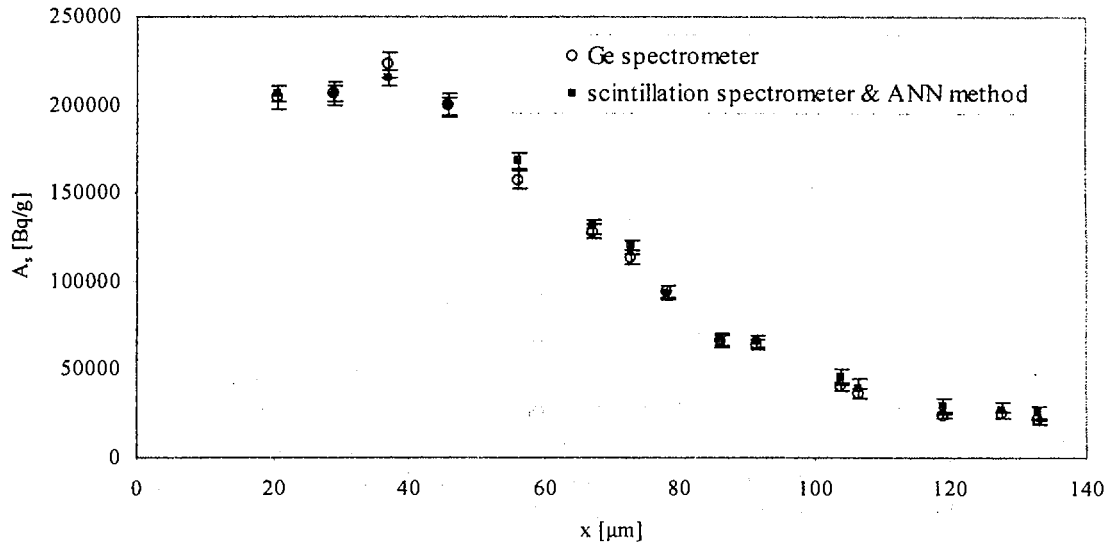


Fig. 4. The results from the Ge spectrometer and from the scintillation spectrometer supported by ANN method

#### 4. TRACERS CONCENTRATION ANALYSIS AND RESULTS

The method presented in chapter 3, allowed evaluation of total activity for each tracer and each sample layer as a function of layer's depth. The total activities were re-calculated to the specific activities  $A_s(x)$  according to the following formula:

$$A_s(x) = \frac{A_T(x)}{\Delta m} \quad (2)$$

where:  $x$  - sample layer depth from the metal surface,  $A_T(x)$  - total activity of tracer in the sample layer,  $\Delta m$  - decrease of sample mass after removing the layer.

In this method the specific activity  $A_s(x)$  is proportional to the tracer concentration  $c(x)$ . At presented experiment the boundary conditions were a semi-infinite solid (metal) and a thin layer of the tracers on metal surface at the diffusion process beginning. The solution of the II Fick's law for tracer concentration distribution is described by the equation (3) where also proportionality between  $c(x)$  and  $A_s(x)$  is shown.

$$A_s(x) \approx c(x) = c_0 \cdot \exp\left(\frac{-x^2}{4D_T t}\right) \quad (3)$$

where:  $t$  - time of the diffusion process,  $D_T$  - diffusion coefficient of the radioactive tracer.

Total amount of the tracer is equal:

$$T = \int_0^{\infty} c(x) dx \quad (4)$$

Combining the equations (3) and (4) the normalized concentration function can be presented at following form:

$$\ln[c(x)/T] = -\frac{1}{4D_T t} \cdot x^2 \quad (5)$$

The above functions are fitted to the experimental data using the software package MATLAB 6.5. The results of fitting are shown in the Figure 5. Poor adjustment of the analytical curve is noticeable in the case of measurements of initially removed layers. Considering the fact that points under discussion cover the thickness of about 20  $\mu\text{m}$ , the adjustment was carried out for the subsequent points. The explanation of the primary points' behaviour is rather difficult. Poor adhesion of the isotopic layer as well as the deformation of the sample surface might be the main source of this error.

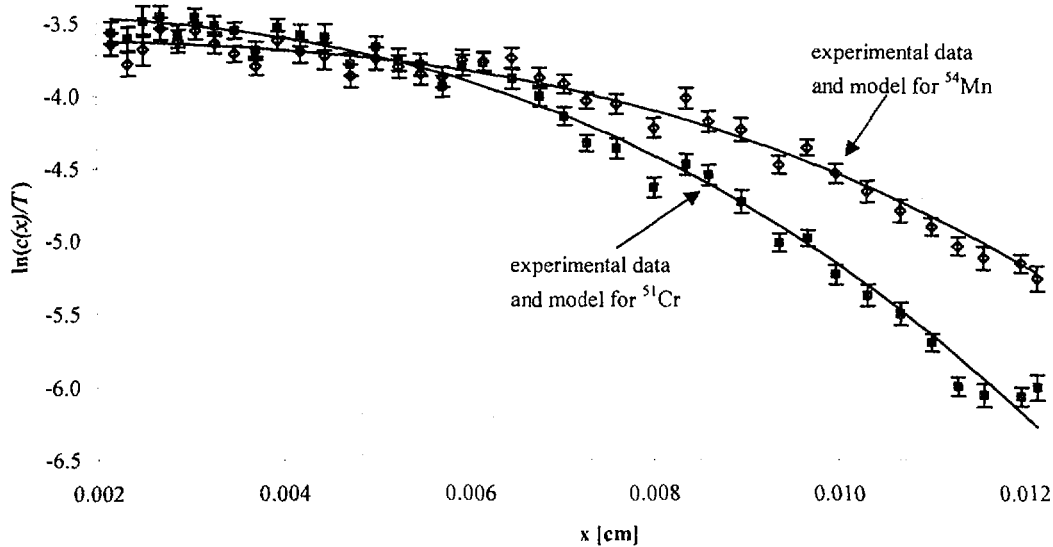


Fig. 5. The experimental data and the models fitted for a 3H13G18S2Ca steel.

The diffusion coefficient of atoms –  $D$ , is related to the one of radiotracer –  $D_T$ , by the following formula:

$$D = \frac{D_T}{f} \quad (6)$$

where  $f$  - correlation factor. It is influenced by the crystal structure and the mechanism of diffusion. For the cubic, face centered crystal structure its value equals 0,78146 [6]. The values of self-diffusion coefficients of metals are listed in Table 2.

Table 2. Diffusion coefficients of metals in the studied Cr-Mn steels

The metal	$D_{Cr}$ [cm <sup>2</sup> s <sup>-1</sup> ]	$D_{Mn}$ [cm <sup>2</sup> s <sup>-1</sup> ]	$D_{Fe}$ [cm <sup>2</sup> s <sup>-1</sup> ]
5H17G17	$(8,11 \pm 0,36) \cdot 10^{-12}$	$(12,78 \pm 0,69) \cdot 10^{-12}$	$(7,77 \pm 0,45) \cdot 10^{-12}$
3H13G18S2Ca	$(11,08 \pm 0,84) \cdot 10^{-12}$	$(19,32 \pm 1,92) \cdot 10^{-12}$	$(11,03 \pm 0,96) \cdot 10^{-12}$

## 5. DISCUSSION

The diffusion rates of chromium and iron are comparable and lower than that of manganese. The diffusion rate of metals is higher in the 3H13G18S2Ca steel, containing Si and Ca. The faster transport of manganese partly explains the morphological structure of the scale that is mainly built of the manganese compounds. Moreover, the depletion of manganese close to the metal/scale interface causes the phase transformation from austenitic to ferritic structure and causes the decrease of the diffusion rate [7]. As it was mentioned above, the dominant components of the scales formed on Cr-Mn steels in SO<sub>2</sub> are MnO and MnCr<sub>2</sub>O<sub>4</sub> spinel. The diffusion coefficients of Cr, Mn and Fe in MnCr<sub>2</sub>O<sub>4</sub> spinel were not found. However, the diffusion coefficient of Mn in MnO is about 10<sup>-9</sup> cm<sup>2</sup>s<sup>-1</sup> at 1173 K [8], higher than that in steel. Hence, it is possible that the transport in the metal phase is the slowest partial process determining the corrosion rate.

## CONCLUSIONS

- The ANN method for multitracer experiment has been developed and applied.
- The lattice diffusion is the dominant mechanism of metals' transport.
- The diffusion rates of Fe and Cr are comparable and lower than the diffusion rate of Mn.
- The diffusion rate of metals is higher in the 3H13G18S2Ca steel, containing Si and Ca.
- Faster depletion of Mn in the near metal/scale region causes the phase transformation from austenitic to ferritic structure. In consequence the oxidation rate of the steels decreases.

## Acknowledgements

This work was supported by the State Committee for Scientific Research.

## References

- [1] Z. M. Jarzębski, Dyfuzja w metalach i stopach, Wydawnictwo „Śląsk”, Katowice 1988
- [2] P.G. Shewmon, Diffusion in Solids, New York 1963
- [3] S. J. Rothman, The Measurements of Tracer Diffusion Coefficients in Solids, in G. E. Murch, A. S. Nowicki (Eds), Diffusion in Crystalline Solids, Academic Press, New York 1984
- [4] A. A. Żuchowicki, A. J. Geodakjan, Żurnal Fizycznej Chymii, 1334, 29, nr 7 (1955)
- [5] Z. Stęgowski, Spektrometryczna analiza widma z detektora scyntylacyjnego z zastosowaniem sztucznych sieci neuronowych, Raporty IChTJ, seria A nr 2/2002, Tom 2, str.484-490, Warszawa 2002
- [6] S. Mrowec, T. Werber, Korozja gazowa tworzyw metalicznych, Wydawnictwo „Śląsk”, Katowice 1965
- [7] J. Łaskawiec, Zeszyty Naukowe P.Ś., seria Hutnictwo, 31, Gliwice 1988
- [8] J. S. Kirkaldy, P. N. Smith, R. C. Sharma, Metall. Trans. 4, 2, 624 (1973)